Communication

Mn-Depleted Zone Formation in Rapidly Cooled High-Strength Low-Alloy Steel Welds

YONGJOON KANG, KYUTAE HAN, JOO HYUN PARK, and CHANGHEE LEE

The mechanism of formation of an Mn-depleted zone (MDZ) near the inclusion in a steel weld was elucidated based on quantification of MDZ depth and thermodynamic calculations. The effective inclusion phase for intragranular nucleation, which increased as a function of increasing chemical driving force, satisfied the requirements for presence of a considerable quantity of Mn in the phase, and a lower precipitation temperature compared with the solidus temperature of the matrix.

DOI: 10.1007/s11661-014-2470-3

Acicular ferrite, the result of the transformation product of intragranular nucleation on inclusions, is recognized as an essential microstructure in steel welds ensuring both strength and impact toughness.[1,2] A number of researchers have proposed mechanisms for acicular ferrite nucleation on the surface of inclusions, including (1) classical heterogeneous nucleation,[3] (2) small lattice misfit between the inclusion and ferrite,[4,5] (3) small interfacial energy between the inclusion and ferrite,[6] (4) solute depletion of the austenite matrix near the inclusion,[4,7–13] and (5) thermal strain due to the difference in thermal expansion between the inclusion and austenite.[14] Babu[15] evaluated these mechanisms, taking into account the similarity between bainite and acicular ferrite transformations, and concluded that an increase of chemical driving force due to the solute depletion is one of the most probable mechanisms of intragranular nucleation. In addition, a number of studies have demonstrated significant similarity between bainite and acicular ferrite transformation.[16–18] Solute depletion (especially Mn-depletion) has been independently verified by several studies using wrought steels deliberately inoculated with selected inclusions.[4,8,10,11] Furthermore, an Mn-depleted zone (MDZ) was recently shown to contribute to the formation of acicular ferrite, not only in wrought steels, but also in steel welds.[12,13]

YONGJOON KANG and KYUTAE HAN, Ph.D. Candidates, and CHANGHEE LEE, Professor, are with the Division of Materials Science and Engineering, Hanyang University, Seoul 133-791, Republic of Korea. Contact e-mail: chlee@hanyang.ac.kr JOO HYUN PARK, Professor, is with the Department of Materials Engineering, Hanyang University, Ansan 426-791, Republic of Korea.

Manuscript submitted February 4, 2014.
Article published online July 22, 2014

The mechanism of formation of MDZ in wrought steels is reportedly due to Mn-absorption of Ti_2O_3 inclusions, which can be achieved by high temperature austenitization heat treatment for several minutes.[4,8,10,11] However, in steel welds, the Mn-absorption phenomenon is not sufficient to explain MDZ formation because the welding thermal cycle appears to provide an insufficient amount of time for Mn-absorption to occur due to the rapid cooling rate and very short dwell time at peak temperature. Therefore, the aim of the present study was to investigate the mechanism of MDZ formation in steel welds.

Two weld metals with or without an MDZ were prepared by controlling the Ti content in the welding wire. Specifically, the Ti contents of the weld metals were 0.007 and 0.17 wt pct, and the specimens were labeled as L (low Ti) and H (high Ti), respectively (Table I). In our recent study,[13] we confirmed that the inclusions in weld metal containing 0.007 wt pct Ti have a good potency for intragranular nucleation, and the MDZ that develops near these inclusions contributes greatly to good potency, while those in weld metals containing 0.17 wt pct Ti have a poor potency for intragranular nucleation with no MDZ around the inclusions. We employed a gas metal arc welding process, and multiple welding passes were deposited in the V-groove of a steel plate with a heat input of approximately 2.0×10^3 kJ/m for each pass. Only the last deposited bead was investigated in order to exclude the reheating effect of subsequent thermal cycles in multi-pass welding.

Microstructures were examined using transmission electron microscopy (TEM) (JEM-2000, JEOL). The phase distribution in a multiphase inclusion and the Mn distribution from the inclusion/matrix interface to the bulk matrix were investigated using elemental mapping and line scanning with a scanning TEM (STEM) (JEM-2100F, JEOL) with energy-dispersive spectrometry (EDS). In order to quantify the depth of the MDZ from the line scanning analysis, the concentration difference (delta) of Mn was measured between the average value within 10 nm from the inclusion/matrix interface and the average value more than 100 nm from the inclusion/matrix interface. Five line scans were carried out to allow computation of an average Mn weight percent difference. High resolution electron microscopy (HREM) images were analyzed and fast Fourier transformation (FFT) patterns were assessed by image analysis software (DigitalMicrograph, Gatan).

The commercial thermochemical computing package FactSage™ (version 6.3) was used to predict the phase formation sequence of multiphase inclusions in conjunction with the transformation of the matrix based on the Gibbs free energy minimization principle using FToxid and FSstel databases. FactSage™ software is widely used for predicting inclusion (oxide/sulfide/nitride)-steel multiphase equilibria.[19–21]

As evidenced in Figure 1, inclusions in weld L were effective for intragranular nucleation, while inclusions in weld H were not effective. Figure 2 shows the EDS elemental maps taken from a typical inclusion of weld L and from that of weld H. Three major components,

Table I. Chemical Composition of Weld Metals (Weight Percent)

Weld	C	Si	Mn	Ni	Cr	Mo	P	S	Al	Ti	B	N	O
L	0.08	0.56	2.3	2.6	1.06	0.57	0.014	0.007	0.022	0.007	0.0007	0.0054	0.0359
H	0.06	0.31	1.7	2.9	0.33	0.47	0.015	0.007	0.021	0.170	0.0006	0.0047	0.0227

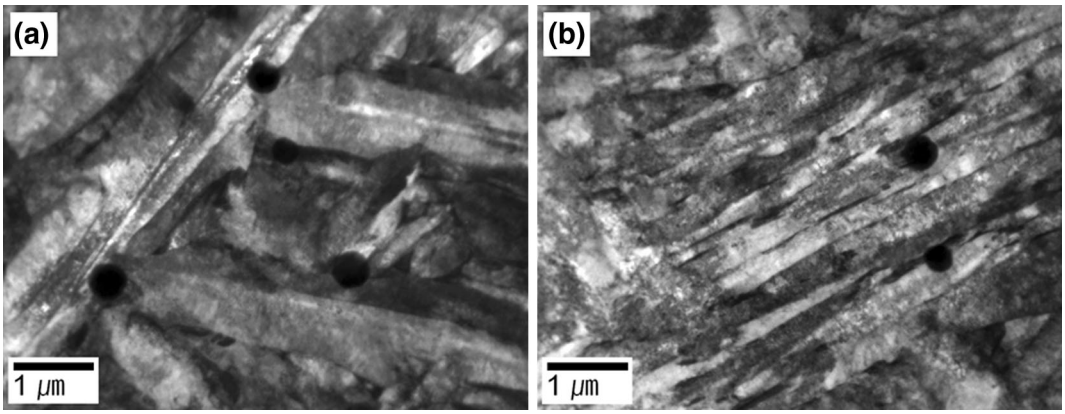

Fig. 1—TEM micrographs of (*a*) weld L and (*b*) weld H.

MnS, Mn-Ti oxide, and Mn-Si oxide, were found in a typical inclusion from weld L (Figure 2(a)). Conversely, a typical inclusion from weld H was mainly composed of Ti oxide with minor amounts of Al-Ti oxide and MnS (Figure 2(b)). Based on our recent study,[13] the Mn-Ti oxide in weld L and the Ti oxide in weld H were identified as $MnTi_2O_4$-rich spinel and Ti_2O_3-rich ilmenite, respectively. The Mn-Si oxide was also confirmed to be in an amorphous phase. Most of the Mn-Si oxide was surrounded by a Ti-rich thin layer (Figure 2(a)). A crystallized Ti-rich layer on the surface of the amorphous Mn-silicate of the inclusion in steel welds has been reported by many researchers.[5,12] Electron energy loss spectroscopy analysis indicated that this layer was consistent with a specific type of Mn-Ti oxide,[12] although its crystal structure has not yet been clearly identified. Figure 3(a) shows an HREM image of a Ti-rich layer on the Mn-silicate surface, while Figures 3(b) and (c) show the analyzed FFT patterns taken from the matrix only (Region 1) and from the matrix with a Ti-rich layer (Region 2), respectively. The d-spacing measured in the Ti-rich layer was approximately 2.145 Å, which corresponded to the space between the {400} plane of $MnTi_2O_4$. Based on the FFT analysis, the Ti-rich layer shown in Figure 2(a) was identified as $MnTi_2O_4$, which was one of the three major components in a typical inclusion of weld L.

Recently, the MDZ around inclusions in steel welds has been shown to contribute considerably to intragranular nucleation.[12,13] However, the mechanism of formation of MDZ in steel welds is not yet fully understood. We previously hypothesized that MDZ formation in steel welds may be due to a combination of the consumption of Mn in the matrix/inclusion interfacial boundary layer to form inclusions containing high amounts of Mn, whose limited homogenization is due to the rapid cooling rate.[13] To evaluate this hypothesis in the present study, we aimed to predict the inclusion formation temperature. To this end, the formation temperature of each non-metallic compound during solidification was predicted based on thermodynamic calculations as shown in Figure 4. In weld L (Figure 4(a)), spinel (a solid solution of $MnTi_2O_4$ and $MnAl_2O_4$) and MnS were calculated to be stable below the solidus temperature of the matrix, while in weld H (Figure 4(b)), the ilmenite (predominantly Ti_2O_3 which dissolves small amounts of $MnTiO_3$) was expected to precipitate above the solidus temperature of the matrix. It could also be inferred from the shape of the interphase boundary between the inclusion and matrix that some facets were present in weld L, while no facets were detected in weld H (Figure 2). Some of the predicted compounds, such as corundum (mainly Al_2O_3), pseudobrookite (mainly Ti_3O_5), and $MnAl_2O_4$ spinel, were not observed in any of experiments, and thus may have originated from kinetic factors during solidification of the weld pool. The results shown in Figure 4(a) implied that a combined effect of the high Mn content and the low precipitation temperature of the inclusion phases (*i.e.*, spinel, MnS) in weld L led to MDZ formation near the inclusions. In other words, once an inclusion containing high amounts of Mn (*i.e.*, spinel, MnS) precipitated during rapid solidification, the Mn in the matrix/inclusion interfacial boundary layer was consumed and depleted. Moreover, as the precipitation temperature decreased less than the solidus temperature of the matrix, the depleted region was considered to have a limited chance to homogenize not only due to the low diffusivity in the austenite matrix, but also due to rapid cooling. On the other hand, Figure 4(b) shows that the homogenization of Mn was predicted to be very fast because the matrix was thought to be in a liquid

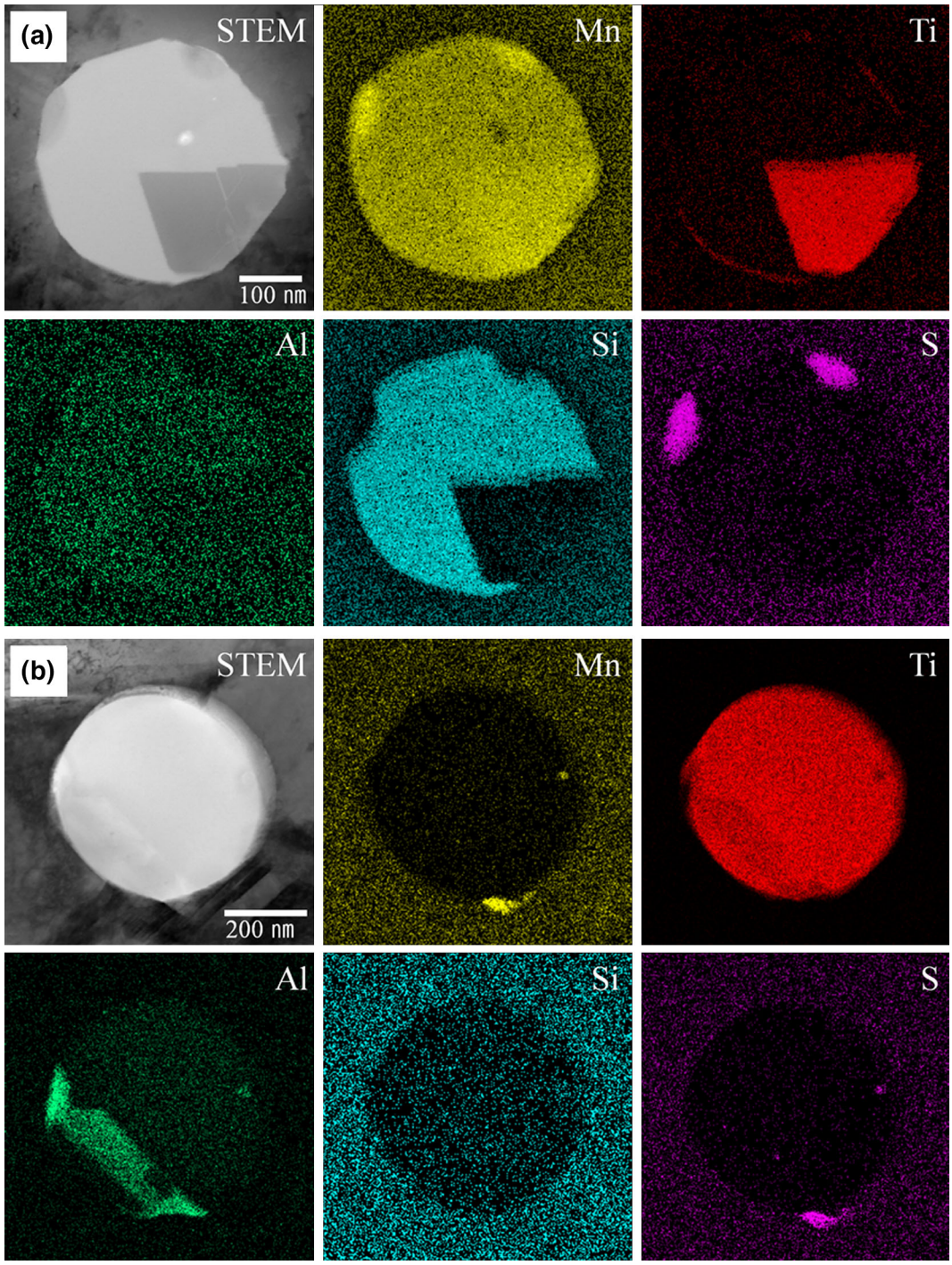

Fig. 2—STEM images and EDS elemental mapping images of inclusions in (*a*) weld L and (*b*) weld H.

phase under the temperatures at which the ilmenite was formed. Furthermore, as the ilmenite in weld H was mainly Ti_2O_3 and had little Mn content, there was very little consumption of Mn in the matrix near the inclusion as ilmenite formed. Thus, two factors described in our recent study[13] were confirmed as possibilities regarding the formation of MDZ: (1) presence of a considerable amount of Mn in the inclusion phase and (2), a lower precipitation temperature than the solidus temperature of the matrix.

In order to corroborate the two factors described above, we evaluated the effect of the precipitation temperature of Mn-containing inclusion phases on the formation of MDZ. The depth of MDZ at the vicinity of each inclusion phase in weld L was quantitatively analyzed by EDS line scanning as shown in Table II. In weld L, the spinel phase was expected to precipitate at a lower temperature of 1511 K (1238 °C) compared with the MnS precipitation temperature of 1713 K (1440 °C), as shown in Figure 4(a). The absolute average depth of

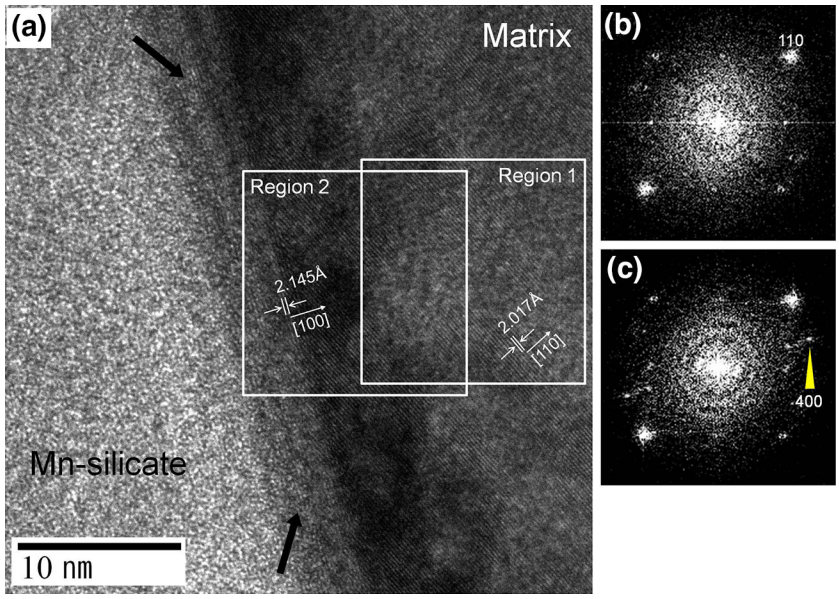

Fig. 3—(*a*) HREM image of the interface between the inclusion and matrix (black arrows indicate the Ti-rich layer), (*b*) FFT patterns taken from Region 1, and (*c*) FFT patterns taken from Region 2.

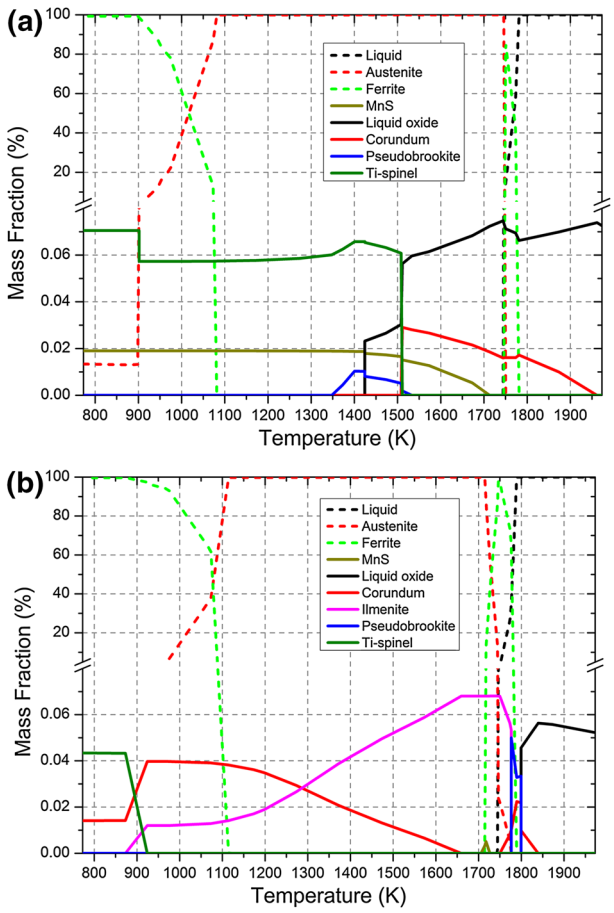

Fig. 4—Calculated mass fraction of the individual phases in welds as a function of temperature. Dashed and straight lines indicate the matrix phases and the inclusion phases, respectively. Note the broken y-axis between 0.1 and 0.2: (*a*) weld L and (*b*) weld H.

the MDZ weight percent difference of Mn increased as the formation temperature of the inclusion phase decreased, and Mn depletion near the $MnTi_2O_4$-rich spinel was more evident compared to that near MnS. The majority of Mn-silicates were enveloped by a Ti-rich layer, which was identified as $MnTi_2O_4$, and thus Mn depletion near the Mn-silicate appeared to be similar to that near the $MnTi_2O_4$-rich spinel. The diffusivity of Mn in austenite decreases considerably with decreasing temperature. Specifically, the Mn diffusivity (D^{γ}_{Mn})in austenite can be determined by

$$D^{\gamma}_{Mn} = (6.5 \times 10^{-5}\ \mathrm{m^2/s}) \exp\left(-\frac{276\mathrm{kJ/mol}}{RT}\right),$$

where R is the gas constant and T is the absolute temperature.[22] Figure 5 shows the calculated diffusivity of Mn in austenite as a function of temperature. The Mn diffusivity in austenite was confirmed to decrease considerably with decreasing temperature from 2.5×10^{-13} $\mathrm{m^2/s}$ at 1713 K (1440 °C) to 1.9×10^{-14} $\mathrm{m^2/s}$ at 1511 K (1238 °C), the estimated precipitation temperatures of MnS and spinel, respectively. Thus, the region near the $MnTi_2O_4$-rich spinel that was formed at a lower temperature compared with MnS appeared to have a lower chance to homogenize, which may have contributed to maintenance of the MDZ. Therefore, $MnTi_2O_4$-rich spinel in weld L was considered to be effective for MDZ formation, and apparently improved the chemical driving force for intragranular nucleation.

In summary, this work identified the mechanism of formation for MDZ in steel welds. In view of an increase in chemical driving force for intragranular nucleation, the effective inclusion phase satisfied both requirements, namely, presence of a considerable amount of Mn in the phase and a lower precipitation temperature compared

Table II. Weight Percent Difference (Delta) of Mn Between the Matrix Distant from the Inclusion and the MDZ in the Vicinity of Each Inclusion Phase (Weight Percent)

Inclusion Phase	Predicted Precipitation Temperature, [K (°C)]	Average	Standard Deviation
MnS	1713 (1440)	−0.179	0.056
Ti-Spinel (Mainly $MnTi_2O_4$)	1511 (1238)	−0.534	0.151
Ti-Rich Layer (Mainly $MnTi_2O_4$) on Mn-Silicate Surface	1511 (1238)	−0.516	0.120

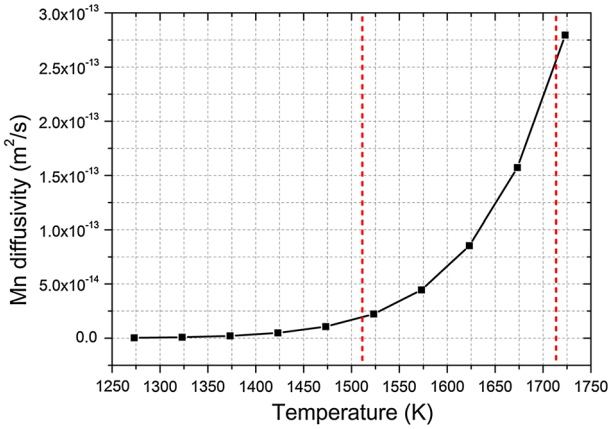

Fig. 5—Calculated diffusivity of Mn in austenite as a function of temperature. The left and right sides of the dashed lines are the precipitation temperature of the spinel and MnS, respectively.

with the solidus temperature of the matrix. Thus, a lower precipitation temperature is better for MDZ formation, indicating that as the Mn-containing inclusion phase forms below the solidus temperature of a matrix; Mn in the diffusion boundary layer is consumed such that the MDZ can develop due to the limited Mn homogenization in the solid state.

This work was supported by the Fundamental R&D Program for the Core Technology of Materials (K0006030, Development of joining materials by the control of phase transformation and critical energy) funded by the Ministry of Trade, Industry & Energy (MI, Korea).

REFERENCES

1. E. Levine and D.C. Hill: *Metall. Trans. A*, 1977, vol. 8A, pp. 1453–63.
2. R.A. Farrar and P.L. Harrison: *J. Mater. Sci.*, 1987, vol. 22, pp. 3812–20.
3. J.M. Dowling, J.M. Corbett, and H.W. Kerr: *Metall. Trans. A*, 1986, vol. 17A, pp. 1611–23.
4. J.M. Gregg and H.K.D.H. Bhadeshia: *Metall. Mater. Trans. A*, 1994, vol. 25A, pp. 1603–11.
5. T. Yamada, H. Terasaki, and Y. Komizo: *ISIJ Int.*, 2009, vol. 49, pp. 1059–62.
6. T. Suzuki, J. Inoue and T. Koseki: *Trends in Welding Research*, Proceedings of the 8th International Conference, p. 292, Pine Mountain, Georgia, 2008.
7. J.M. Gregg and H.K.D.H. Bhadeshia: *Acta Mater.*, 1997, vol. 45, pp. 739–48.
8. J.-H. Shim, Y.W. Cho, S.H. Chung, J.-D. Shim, and D.N. Lee: *Acta Mater.*, 1999, vol. 47, pp. 2751–60.
9. J.-H. Shim, Y.-J. Oh, J.-Y. Suh, Y.W. Cho, J.-D. Shim, J.-S. Byun, and D.N. Lee: *Acta Mater.*, 2001, vol. 49, pp. 2115–22.
10. J.-H. Shim, J.-S. Byun, Y.W. Cho, Y.-J. Oh, J.-D. Shim, and D.N. Lee: *Scripta Mater.*, 2001, vol. 44, pp. 49–54.
11. J.-S. Byun, J.-H. Shim, Y.W. Cho, and D.N. Lee: *Acta Mater.*, 2003, vol. 51, pp. 1593–1606.
12. J.S. Seo, H.J. Kim, and C. Lee: *ISIJ Int.*, 2013, vol. 53, pp. 880–86.
13. Y. Kang, J. Jang, J.H. Park, and C. Lee: *Met. Mater. Int.*, 2014, vol. 20, pp. 119–27.
14. M. Enomoto: *Met. Mater.*, 1998, vol. 4, pp. 115–23.
15. S.S. Babu: *Curr. Opin. Solid State Mater. Sci.*, 2004, vol. 8, pp. 267–78.
16. A.-F. Gourgues, H.M. Flower, and T.C. Lindley: *Mater. Sci. Tech. Ser.*, 2000, vol. 16, pp. 26–40.
17. J.R. Yang and H.K.D.H. Bhadeshia: *J. Mater. Sci.*, 1991, vol. 26, pp. 839–45.
18. S.S. Babu and H.K.D.H. Bhadeshia: *Mater. Sci. Eng. A-Struct.*, 1992, vol. 156, pp. 1–9.
19. J.H. Park and Y.-B. Kang: *Metall. Mater. Trans. B*, 2006, vol. 37B, pp. 791–97.
20. J.H. Park: *CALPHAD*, 2011, vol. 35, pp. 455–62.
21. J.S. Park, C. Lee, and J.H. Park: *Metall. Mater. Trans. B*, 2012, vol. 43B, pp. 1550–64.
22. W.C. Leslie: *The Physical Metallurgy of Steels*, McGraw-Hill, New York, 1982, p. 176.